Published in final edited form as:
Bioconjug Chem. 2006 ; 17(2): 317–326. doi:10.1021/bc0502457.

Polycefin, a New Prototype of a Multifunctional Nanoconjugate Based on Poly(β-L-malic acid) for Drug Delivery

Bong-Seop Lee[†,‡,‖], **Manabu Fujita**[†,‖], **Natalya M. Khazenzon**[†], **Kolja A. Wawrowsky**[†], **Sebastian Wachsmann-Hogiu**[§], **Daniel L. Farkas**[§], **Keith L. Black**[†,⊥], **Julia Y. Ljubimova**[†,⊥], and **Eggehard Holler**[*,‡,⊥]

Institut für Biophysik und physikalische Biochemie der Universität Regensburg, Germany, Maxine Dunitz Neurosurgical Institute, Cedars-Sinai Medical Center, Los Angeles, California 90048, Department of Surgery, Cedars-Sinai Medical Center, Los Angeles, California, and Arrogene, Inc., Tarzana, California 91356.

[†] Maxine Dunitz Neurosurgical Institute, Cedars-Sinai Medical Center.

[‡] Institut für Biophysik und physikalische Biochemie der Universität Regensburg.

[§] Department of Surgery, Cedars-Sinai Medical Center.

[⊥] Arrogene, Inc.

Abstract

A new prototype of nanoconjugate, Polycefin, was synthesized for targeted delivery of antisense oligonucleotides and monoclonal antibodies to brain tumors. The macromolecular carrier contains: 1. biodegradable, nonimmunogenic, nontoxic β-poly(L-malic acid) of microbial origin; 2. Morpholino antisense oligonucleotides targeting laminin α4 and β1 chains of laminin-8, which is specifically overexpressed in glial brain tumors; 3. monoclonal anti-transferrin receptor antibody for specific tissue targeting; 4. oligonucleotide releasing disulfide units; 5. L-valine containing, pH-sensitive membrane disrupting unit(s), 6. protective poly(ethylene glycol); 7. a fluorescent dye (optional). Highly purified modules were conjugated directly with *N*-hydroxysuccinimidyl ester-activated β-poly-(L-malic acid) at pendant carboxyl groups or at thiol containing spacers via thioether and disulfide bonds. Products were chemically validated by physical, chemical, and functional tests. In vitro experiments using two human glioma cell lines U87MG and T98G demonstrated that Polycefin was delivered into the tumor cells by a receptor-mediated endocytosis mechanism and was able to inhibit the synthesis of laminin-8 α4 and β1 chains at the same time. Inhibition of laminin-8 expression was in agreement with the designed endosomal membrane disruption and drug releasing activity. In vivo imaging showed the accumulation of intravenously injected Polycefin in brain tumor tissue via the antibody-targeted transferrin receptor-mediated endosomal pathway in addition to a less efficient mechanism known for high molecular mass biopolymers as enhanced permeability and retention effect. Polycefin was nontoxic to normal and tumor astrocytes in a wide range of concentrations, accumulated in brain tumor, and could be used for specific targeting of several biomarkers simultaneously.

[*] Corresponding author. eggehard.holler@biologie.uniregensburg.de. Phone +49 941 943 3030. Fax +49 941 943 2813..
[‖] Two authors contributed equally for this paper.

Note Added after ASAP Publication. In the version of the manuscript posted January 19, 2006, corrections were made to text in the first paragraph of Experimental Procedures and the last paragraph of Results. The corrected version of the manuscript was posted January 25, 2006.

INTRODUCTION

Targeted delivery of drugs reduces systemic toxicity and increases the drug concentration at the tumor site. It can be achieved by specific multicomponent nanoscale devices such as liposomes, particles, and nanoconjugates (1–3). High-molecular-mass nanoconjugates based on water-soluble macromolecules offer several advantages over direct delivery of drugs: 1. Delivery of both lipophilic and hydrophilic drugs, in particular, of antisense oligonucleotides, through biological barriers such as the blood–brain barrier (4, 5); 2. Delivery of a multitude of different drugs by each single carrier molecule allowing synergism in recipient cells (6, 7); 3. Targeting of a drug delivery device to tumors with minimal damage to healthy tissue; 4. Targeting to tumor cells due to an enhanced permeability and retention (EPR)[1] effect (8–12); 5. Targeting by receptor-mediated binding to surfaces of recipient cells and endosomal uptake into these cells (13–16); 6. Provision of an activity for disruption of endosomal membranes and for the release of the drug carrier system into the cytoplasm (17–22); 7. A cleavable linkage for the release of the drug from the carrier system (23–26); 8. A prolonged circulation through protection by PEG against degradation activities (27–30); and 9. Attachment of a fluorescent reporter for the localization of the carrier system. Available drug delivery systems either do not comply with a complete set of these demands or they have several of these properties but suffer from nonbiodegradability, immunogenicity and toxicity. We designed and synthesized a prototype nanoconjugate intended to fulfill the above criteria and to be used as a future anticancer drug delivery system to brain tumors.

Ideally, a nanoconjugate contains a central scaffold with numerous pendant chemical groups allowing for covalently attaching modules with the above functions. These can be designed to vary in the kind and number of prodrug(s), targeting specificity, and drug releasing activity (endosomal or cytoplasmic). Of the highly developed nanoconjugate delivery systems, scaffolds frequently represent copolymers of substituted acrylic acid, notably *N*-(2-hydroxypropyl)methacrylamide (HPMA) copolymer (31–35). This kind of scaffold, however, suffers from resistance to biodegradation.

We report here on the chemical synthesis of a new nano-conjugate prototype of drug delivery system, by sequential conjugation of functional modules to a nontoxic, nonimmunogenic, biogenic scaffold, β-poly(L-malic acid) (PMLA) (36). This polymer has been highly purified from the myxomycete *Physarum polycephalum*. PMLA resembles HPMA in carrying abundant carboxyl groups, but as a polyester of L-malic acid, it is completely biodegraded to carbon dioxide and water. On the basis of established synthetic methods, we succeeded to chemically conjugate functional modules to the pendant carboxyl groups in a controlled, newly developed manner to form novel nanoscale structures. Specifically, these modules were: 1. The drugs: Morpholino antisense oligonucleotide (MORPH-AON) to laminin α4 and MORPH-AON to laminin β1 chains, 2. The targeting molecule: transferrin receptor monoclonal antibody (mAb OX-26 for rat and mAb R17217 for mouse), 3. The drug releasing module: disulfide bridges between the MORPH-AON and the scaffold (26), 4. The endosome escaping module: hydrophobic stretches of valine or leucine ethyl ester-conjugated scaffold (17–22), 5. The degradation protecting module: PEG (27–30), 6. The optional reporter module: Fluorescein or Alexa Fluor 680.

[1]Abbreviations: EPR, enhanced permeability and retention; HPMA, *N*-(2-hydroxypropyl)methacrylamide; PMLA, β-poly(L-malic acid); MORPH-AON, morpholino antisense oligonucleotide; BTB, blood–tumor barrier; PBS, phosphate-buffered saline; PDP, 3-(2-pyridyldithio)-propionate; MTS, [3-(4,5-dimethylthiazol-2-yl)-5-(3-carboxymethoxyphenyl)-2-(4-sulfophenyl)-2*H*-tetrazolium, inner salt]; RBC, red blood cell; SEC-HPLC, size exclusion-HPLC; DTT, dithiothreitol; 2-MEA, 2-mercaptoethylamine; NHS, *N*-hydroxysuccinimide; RP-HPLC, reversed phase-HPLC; TNBS, trinitrofluorobenzene; DCC, dicyclohexylcarbodiimide; SPDP, *N*-succinimidyl-3-(2-pyridyldithio)propinate; Polycefin(-mAb), Polycefin devoid of mAb.

MORPH-AONs were designed to inhibit the synthesis of α4 and β1 chains of laminin-8, which is overexpressed in vessel walls of highly vascular glial tumors, breast cancer and their metastases (37, 38). This inhibition has been shown to reduce invasion of human gliomas in vitro (39). MORPH-AONs, unlike other oligonucleotides, are resistant against nucleolytic degradation and are highly specific at low concentrations (40). Transferrin receptor antibody was chosen to target the delivery device beyond the blood–tumor barrier (BTB) in brain to the glioma target cells by promoting receptor binding and endosomal uptake (41–45). Targeting to tumor was reinforced by the EPR effect (8–12). The delivery system is based on a biologically produced scaffold and has a complex modular structure.

EXPERIMENTAL PROCEDURES

Reagents Used

Morpholino-3'-NH_2 antisense oligonucleotides AGC-TCA-AAG-CCA-TTT-CTC-CGC-TGA–C to laminin α4 (MORPH-AON-1) and CTA-GCA-ACT-GGA-GAAGCC-CCA-TGC-C to laminin β1 (MORPH-AON-2) (38, 39) chains were custom-made by Gene Tools (Philomath, OR). Mouse anti-rat mAb (clone OX-26, IgG_{2a}, , 1 mg/mL in PBS; cross-reacting with human as shown in this work) and rat anti-mouse mAb (clone R17217, IgG_{2a}, κ, 1 mg/mL in PBS) to transferrin receptor (CD71) were obtained from Chemicon International (Temecula, CA). β-Poly(L-malic acid) (PMLA) (**1**), a natural polymer of molecular mass M_w = 50000 (polydispersity M_w/M_n = 1.3) from the culture broth of *Physarum polycephalum,* was highly purified (36) and size-fractionated on Sephadex G25. The lyophilized polyacid was devoid of material absorbing at 260 and 280 nm wavelengths. If not mentioned otherwise, molar quantities refer to total malyl residues. Chromatographically pure $mPEG_{5000}$-amine and maleimide-PEG_{3400}-maleimide were obtained from Nektar Therapeutics (San Carlos, CA). 3-(2-Pyridyldithio)-propionate (PDP) was synthesized as described (46). Fluorescein-5-maleimide was obtained from Molecular Probes (Leiden, The Netherlands) and Alexa Fluor 680 C_2-maleimide from Molecular Probes-Invitrogen (Karlsruhe, Germany). Endosomal marker FM 4-64 was purchased from Molecular Probes. All other chemicals of highest purity were bought from Merck (Darmstadt, Germany), Sigma-Aldrich (Munich, Germany), and Pierce (Rockford, IL). Glioma cell lines U87MG and T98G were from American Type Culture Collection (Manassas, VA), and normal human embryonic astrocyte cell line HAST040 was obtained from Clonexpress (Gaithersburg, MD).

Cell Lines and Culture Conditions

Two types of human GBM cell lines (T98G and U87MG) were used. Cells were cultured in Eagle's MEM with 10% fetal calf serum, L-glutamine, sodium bicarbonate, nonessential amino acids, antibiotics, and sodium pyruvate. Normal embryonic brain astrocyte cell line HAST040 (Clonexpress) was also used in toxicity assays.

Cell Viability Assay

To measure cell viability, cells were quantified using the CellTiter 96 AQueous One Solution Cell Proliferation Assay kit (Promega Mannheim, Germany) designed for the determination of the number of viable cells with MTS reagent [3-(4,5-dimethylthiazol-2-yl)-5-(3-carboxymethoxyphenyl)-2-(4-sulfophenyl)-2*H*-tetrazolium, inner salt]. Protocols supplied by the company were exactly followed. A_{490} was recorded on a Spectra Max Plus 384 ELISA reader (IBB, Atlanta, GA). Concentration of Polycefin equal to 1.4 μM corresponds to the concentration of MORPH-AONs of 2.5 mg/kg. It is the working concentration recommended for antisense nucleotides to block mRNA synthesis in vitro and in vivo (47).

In Vivo Fluorescence Imaging

Xenogen IVIS 200 imaging system (Xenogen, Alameda, CA) was used on whole body and isolated organs of glioma-bearing mice 6–72 h following Polycefin injection and after PBS organ/body perfusion to remove the fluorescent drug from circulation. For imaging experiments on mice, Polycefin with attached L-leucine ethyl ester instead of L-valine, with rat mAb R17217 to mouse transferrin receptor and Alexa Fluor 680 dye. The excitation wavelength for the dye was 660 nm. Images were acquired and analyzed at 3.9 cm (organs) or 13 cm (whole mouse) field of view using Living Image Software 2.50. In preliminary experiments, a proprietary MISTI imaging system equipped with 20 nm bandwidth interference filter (ChromaTech) and emission wavelength 700 nm was used. Both imaging systems produced similar results.

Animals

All surgical and nonsurgical procedures were performed in full accordance with IACUC protocol 001462, obtained in May 2005 at Cedars-Sinai Medical Center and with the tenets of the Declaration of Helsinki.

Nude Mice [Tac:Cr:(MCr)-*Foxn*^{nu} mice], after intraperitoneal anesthesia by ketamine 75 mg/kg and medetomidine 1.0 mg/kg, were used. A 10 mm middle line skin incision was made on mouse's skull. A hole in the skull 2 mm laterally and 1 mm rostrally from the Bregma (sagittal and transverse lines crossing point) was made using a dental drill by aseptic technique. Mice underwent stereotactic intracranial injection of 5×10^4 U87MG human glioma cells to the right basal ganglia field using a 2 μL Hamilton syringe over a period of 1 min.

On day 21 after tumor implantation, the mice underwent the intravenous injection of Polycefin at the concentration of 5 mg/kg (47) dissolved in PBS via the tail vein using a 30-gauge needle 1 mL syringe, at a rate of 100 μL within 5 s.

Confocal Microscopy

A TCS SP spectral scanner (Leica Microsystems, Mannheim, Germany) was used for confocal microscopy. Image stacks of 160 by 160 μm in size and 7.5 μm in depth of live U87MG glioma cells were acquired with a Leica PlanApo 63/1.2 NA lens. Live cells were placed in an Attofluor incubation chamber (Molecular Probes). A temperature of 37 °C was maintained by a separate lens and chamber heating system. The fluorescein derivatives of Polycefin with (**8**) or without (**18**) conjugated transferrin receptor mAb OX-26 were added to cells in serum-free medium at a concentration of 1.4 μM MORPH-AON. Simultaneously with Polycefin, cells received 5 μg/mL (as per the manufacturer's instructions) of lipophilic styryl red fluorescent dye FM 4-64 (Molecular Probes) to visualize endosomes.

Hemolytic Assay

To assess membrane-disrupting activities, hemolytic properties of Polycefin and other conjugates were measured by the red blood cell (RBC) hemolysis assay (21) for 2 nmol of conjugate per 10^8 RBCs after incubation at 37 °C (1 h) in 1.5 mL of 100 mM sodium phosphate buffer at several given pHs. Percent hemolysis $(A - A_o)/(A_{tot} - A_o)$ as averaged over three independent measurements and calculated from A_{541} (= A) of the clear supernatant after pelletting. A_o refers to spontaneous and A_{tot} to complete hemolysis in distilled water.

Western Blot Analysis

Reducing SDS–PAGE (with 20 mM DTT) on 10% polyacrylamide gels (samples boiled for 5 min in 5% SDS) and routine Western blotting were carried out as published (39).

Polycefin (**8**) at a concentration of 1.4 μM MORPH-AON (38) was added to the medium of human glioma U87MG and T98G cultures on day 1 and 4 in culture media. For the detection of laminins, serum-free conditioned medium was sampled at day 6 from culture supernatants above equal numbers of cells that has been cultured for the same period of time. Samples were concentrated 10-fold by filtering through Centriplus filtration devices (Millipore, Bedford, MA) and proteins were separated using Tris-acetate 3–8% gradient SDS–PAGE (Invitrogen) under reducing conditions. Lysates of human glioma T98G, known to express laminin-8 (48), were used as a positive control. The gels were blotted onto nitrocellulose membrane (Invitrogen). The membranes were probed with mAbs followed by chemiluminescent detection using the Immune-Star kit with alkaline phosphatase-conjugated secondary antibodies (Bio-Rad Hercules, CA). Antibodies were used to laminin α4 [mAb 8B12 (48)] and β1 chains (mAb LT3). Antibody to human fibronectin 8th type III repeat [mAb 568 (39)] was used to control for equal loading of gel lanes.

Densitometric Analysis

The intensities of the bands of interest after Western blot analysis were determined using the AlphaImager 2000 densitometer (Alpha Innotech, Inc., San Leandro, CA) and expressed relative to the fibronectin band intensities for the same specimens. Background was subtracted from each reading before determining the intensity ratios.

Test of the Morpholino Oligonucleotides Releasing Module of Polycefin

To demonstrate the activity of the oligonucleotide releasing module, Polycefin (0.25 mM bound MORPH-AONs) was incubated with 3 mM GSH (γ-L-glutamyl-L-cysteinylglycine) in 50 mM phosphate buffer pH 7.4 at 37 °C. Samples at various times were stopped with 20 mM *N*-ethylmaleimide, and the liberated reduced oligonucleotide was detected as the *N*-ethylmaleimidyl derivative by SEC–HPLC, A_{260}. 100% release was measured in the presence of 50 mM dithiothreitol (DTT) (60 min, 37 °C).

Analytical Chemical Methods

Thiol residues of conjugates were assayed by the method of Ellman after removal of free 2-MEA by diafiltration (5 kDa cutoff). Amounts of maleimido groups were quantified by their reaction with a given amount of 2-MEA. During the preparation of PMLA conjugates, the substitution of *N*-hydroxysuccinimidyl (NHS) residues was followed by RP-HPLC analysis of the reaction mixtures. Amino acids were quantified by RP-HPLC after hydrolysis of conjugates in 6 M HCl at 100 °C and colorimetry with trinitrofluorobenzene (TNBS) following standard protocols.

Instrumentation

^{1}H NMR spectra were recorded on a Bruker Model DMX-500 Fourier transform spectrometer with MTS as internal standard. Chromatography was performed on a Merck-Hitachi (Ghent, Belgium) analytical LaChrom D-7000 HPLC-UV and fluorescence detector system with either Macherey & Nagel (Düren, Germany) C_{18}-Nucleosil reversed phase RP (250/4 mm) or size exclusion Bio-Sil SEC 250-5 (5 μm, 300/7.8 mm) columns. Molecular mass markers were polysty-rene sulfonates from Machery-Nagel and proteins from Sigma-Aldrich. Merck precoated silica gel 60 F_{254} aluminum sheets were used in thin-layer chromatography with *n*-butanol, water, and acetic acid (4:2:1 by volume) as solvent.

Synthesis of Polycefin. Synthesis of Intermediates and Conjugates

Polycefin, fluorescent dye-Polycefin, and other conjugates have been synthesized from the following intermediates (Scheme 1):

PMLA-N-hydroxysuccinimidyl Ester (PMLA-NHS) (2)—A mixture of anhydrous 10 mmol PMLA (**1**), *N*-hydroxysuccinimide (NHS), and dicyclohexylcarbodiimide (DCC) (15 mmol) in DMF was incubated at room temperature. Dicyclohexylurea was exhaustively removed and product precipitated with ethyl acetate (P1), diethyl ether (P2), and *n*-hexane (P3) in this order. Products P1–P3 were dissolved in DMF, purified over Sephadex LH 20, and then stored as precipitates at –20 °C. PMLA-NHS ester was assayed by exhaustive reaction with *n*-butyl-amine and analysis of free NHS by RP-HPLC [aqueous 0.1% (v/v) TFA] recording A_{260} with reference to NHS standards. Contents were 35, 59, and 85% for P1, P2, and P3 (percentage refers to total PMLA-malyl residues). For the synthesis of Polycefin, P3 was used. Its overall yield was 50–60% with regard to input PMLA. ^{1}H NMR spectra of PMLA-NHS ester in $(CD_3)_2SO$ indicated chemical shifts at 2.8 ppm (singulet, 4H, N–CO–CH_2), 3.35 ppm (doublet, the methylene protons of the polyester backbone), and 5.85 ppm (triplet, the methine protons of the polyester backbone).

(2-Pyridyldithio)propionyl Morpholino Antisense Oligonucleotides (PDP–MORPH-AONs) (conjugates 6-α4 and 6-β1 in Scheme 1)—Morpholino-3'-NH_2 oligonucleotide was coupled in 10% aqueous DMF with *N*-succinimidyl-3-(2-pyridyldithio)-propionate (SPDP) (2-fold excess, 20 °C). After passage over a Sephadex G-25 microspin column in 0.1 M sodium phosphate buffer (pH 6.5), 0.15 M NaCl, and 10 mM EDTA (Buffer A), the product was pure by TLC. The PDP-content was assayed by RP-HPLC after reaction with dithiothreitol (DTT). 2-Thiopyridone was detected at 341 nm wavelength and its concentration measured against reduced 2-aldrithiol as a standard. Yields were >80%.

mAb OX-26-(S-succinimidyl-PEG$_{3400}$-maleimide)$_3$ (conjugate 4 in Scheme 1)—MAb OX-26 (20–30 nmol) or mAb R17217 was reduced in the presence of 53 μmol of solid 2-MEA hydrochloride in Buffer A (90 min at 37 °C). The product was washed over Sigma Ultrafree-CL microcentrifuge filters (30 kDa cutoff) to remove free 2-MEA (tests with Ellman's reagent). Free sulfhydryls were reacted with a 50-fold excess of male-imide-PEG_{3400}-maleimide over antibody, and excess reagent was removed by diafiltration (50 kDa cutoff). Purity was controlled by SEC–HPLC. Positions were 7.20–7.26 min for conjugate **4** and 13.4–13.7 min for maleimide-PEG_{3400}-maleimide. Of the thiol groups, 3.1–3.5 were detected in reduced antibody, and of the maleimido groups, 2.7–3.0 were detected in conjugate **4**, suggesting the formula mAb OX-26-(*S*-succinimidyl-PEG_{3400}-maleimide)$_3$ in Scheme 1.

PMLA/mPEG$_{5000}$-NH$_2$ (5%)/2- MEA (10%)/valine (49%) (conjugate 3 in Scheme 1) and Other Conjugates—The symbol "/" refers to conjugation of the indicated moiety with PMLA. PMLA-NHS esters dissolved in DMF were conjugated with mPEG$_{5000}$-NH_2, 2-MEA, and L-valine (or gylcine and L-alanine) by amide formation in this order. Specifically, PMLA-NHS P3 (1 mmol) was conjugated with 50 μmol mPEG$_{5000}$-NH_2 at 5% of the malyl residues (100% = all malyl groups in the preparation), followed by conjugation with 100 μmol of 2-MEA at 10% of the malyl residues. Completeness of each reaction was assayed by TLC and tested with ninhydrin. No precipitates were observed that could have affected stoichiometries. Finally, 1 mmol of L-valine (or glycine, L-alanine) was conjugated in DMF/PBS (a mixture of equal volumes) for 1 h at 20 °C. Again, no precipitate was observed. The product was transferred to Buffer A by solvent evaporation/complete resolubilization containing 0.5 mM DTT and purified over Sephadex G25 column.

Lyophilized fractions were used in the synthesis of Polycefin. The composition of conjugate **3** was PMLA, $mPEG_{5000}$ (5%), 2-MEA (10%), and L-valine (49%). Each of the reactions was completed except for the amino acids, which were assayed after conjugation, validating the given composition. To measure effects of various conjugated groups (for instance on membrane stability by the hemolysis assay), additional conjugates were synthesized: **9** PMLA/$mPEG_{5000}$ (5%)/2-MEA (5%), **10** PMLA/$mPEG_{5000}$ (10%)/2-MEA (5%), **11** PMLA/$mPEG_{5000}$ (15%)/2-MEA (5%), **12** PMLA/$mPEG_{5000}$ (5%)/2-MEA (5%)/glycine (63%), **13** PMLA/$mPEG_{5000}$ (5%)/2-MEA (5%)/L-alanine (56%), **14** PMLA/$mPEG_{5000}$ (5%)/2-MEA (5%)/L-valine (55%), **15** PMLA/$mPEG_{5000}$-NH_2 (5%)/2-MEA (10%)/valine (15%), **16** PMLA/$mPEG_{5000}$-NH_2 (5%)/2-MEA (10%)/valine (34%), **17** PMLA/$mPEG_{5000}$-NH_2 (5%)/2-MEA (10%)/valine (55%), **18** PMLA/$mPEG_{5000}$-NH_2 (5%)/2-MEA (10%)/valine (50%)/(2-pyridyldithio)propionyl-morpholino AON to laminin α4 chain (2.5%)/(2-pyridyldithio)propionyl-morpholino AON to laminin β1 chain (2.5%)/3-(2-pyridyldithio)propionate, **19** PMLA/$mPEG_{5000}$-NH_2 (5%)/2-MEA (10%)/valine (50%)/mAB-(*S*-succinimidyl-PEG_{3400}-maleimide)$_3$ (0.23%)/3-(2-pyridyldithio)-propionate, **20** Polycefin variant with leucine ethyl ester instead of valine, with mAb R17217 to mouse, and with Alexa Fluor 680, **21** as for **20**, but without mAb. Free sulfhydryl groups were blocked with 3-(2-pyridyldithio)propionate (PDP).

Synthesis of Dye-Polycefin (7 in Scheme 1) and Polycefin (8)—Freshly prepared mAb OX-26-(*S*-succinyl-PEG_{3400}-maleimide)$_3$ (conjugate **4**) was added dropwise to conjugate **3** dissolved in Buffer A at 4 °C. Free thiol groups (conjugate **3**) were in 50-fold excess over maleimido groups (conjugate **4**). Next, 2.5 μmol of fluorescein-5-maleimide or Alexa Fluor 680 C_2-maleimide (compounds **5**), 5 μmol of PDP–Morph-AON1 (**6**-α4), and 5 μmol of PDP–Morph-AON2 (**6**-β1) were coupled overnight to the growing conjugate. To obtain Polycefin (**8**), the conjugation with **5** was omitted. Completeness of the reactions was indicated by a single peak after SEC–HPLC. Unreacted free sulfhydryl groups were blocked with 3-(2-pyridyldithio)propionate (PDP). The obtained conjugates **7** and **8** were purified by diafiltration (100 kDa cutoff) and lyophilized. The absolute yields were 75–80% with reference to conjugate **3** (100%), and the overall yield with reference to PMLA (**1**) input was 25%. For cell delivery and membrane disruption studies, conjugates resembling Polycefin, **18** either without mAb OX-26 or **19** without the oligonucleotides, and for imaging experiments, Polycefin variants **20** and **21**, were synthesized and purified by analogous methods.

RESULTS

Synthesis of Polycefin

The nanoscale synthesis of Polycefin outlined in Scheme 1 and described under Experimental Procedures afforded the highly controlled chemical coupling of macromolecular groups (modules) with the polymeric PMLA scaffold. In the beginning, the scaffold carboxyl groups were activated by forming *N*-hydroxysuccinimidyl esters of the polymer (PMLA-NHS) that were then substituted by PEG_{5000}-NH_2, 2-mercaptoethylamine (2-MEA), and L-valine in forming amide bonds with the carboxylates. The reactions were sequential without purification of intermediates. Products were validated by demonstrating complete consumption of the substituting amines and correlation with the released amount of NHS. Only the coupling of amino acids caused a small fraction of spontaneous hydrolysis of PMLA-NHS. The stoichiometry for valine and the other amino acids was derived from quantitative amino acid analysis. The multiple conjugate thus obtained (conjugate **3** in Scheme 1) contained 33–35% free carboxylates.

Probing PMLA and PMLA-NHS by SEC–HPLC indicated a dramatic change in conformation by the esterification from a probably extended to a compact structure in aqueous solution. The consequently decreased solubility in water was improved by conjugation of PEG_{5000}, which also should confer stability in body fluids (27–30). Only after conjugation of PEG, the pending thiol groups of conjugate **3** became accessible to the reactions with mAb OX-26 (or mAb R17217) and MORPH-AONs.

The reactions with mAb OX-26 or mAb R17217and MORPH-AONs required mild conditions in order to avoid irreversible denaturation. The conjugation of mAb involved at first a reduction of disulfide bridges resulting in the formation of 3 thiol residues per antibody and reaction with excessive male-imide-PEG_{3400}-maleimide forming the conjugate **4** (Scheme 1). The free unreacted maleimido groups were reserved to substitute at thiols of scaffold-bound 2-MEA (in conjugate **3**) forming thioether conjugates. SEC–HPLC and nonreducing SDS–PAGE prior to this conjugation indicated molecular masses of 150 kDa for both the reduced mAb and PEG-mAb, consistent with single mAb conjugates of maleimide-PEG_{3400}-maleimide (results not shown).

The cleavage site for the release of the MORPHAONs from the carrier was constructed as an interspacing disulfide group between MORPH-AON and 2-MEA on the scaffold. This allowed the reductive cleavage by glutathione in the target cell cytoplasm. The disulfide was introduced by the disulfide exchange reaction of 2-MEA-thiol groups, bound to the scaffold, with PDP-MORPH-AONs (conjugates **6** in Scheme 1).

Polycefin and dye-Polycefin were assembled by the consecutive chemical coupling of the scaffold conjugate **3** with modules **4**, **5**, and **6** (Scheme 1). Their controlled synthesis together with their chromatographic and chemical characterization validated their structural composition, chemical functionality, and purity. At a 50-fold molar excess of thiol residues in conjugate **3** over conjugate **4**, the reaction with mAb was quantitative implicating an average of one molecule of antibody bound per molecule of scaffold. The covalent attachment of MORPH-AONs (conjugates **6**) was quantitative as verified by SEC–HPLC of educts and products.

Properties of Polycefin

The structure of dye-Polycefin is shown in Scheme 1 (in Polycefin, the dye module **5** is substituted by 3-thiopropionic acid). PMLA constitutes a scaffold that can bind a deliberate number of functional modules allowing versatile tissue-specific drug vehicles. The modules are statistically distributed over the scaffold at the abundances given in Scheme 1 in percentages of total malyl residues. The homogeneity of the scaffold-forming PMLA is characterized by its natural polydispersity. On the basis of a M_w of 50000 (corresponding to approximately 500 malyl residues), Polycefin molecules contain on average 1 molecule of mAb (targeting module), 11 molecules of conjugate **6**-α4, 11 molecules of conjugate **6**-β1, 22 molecules of $mPEG_{5000}$ (protecting module), 210–220 molecules of L-valine (membrane disrupting module), and 140–150 pending carboxylate residues. The composition accounted for a molecular mass of approximately 550000. The stoichiometry of 1:20–1:26 mAb relative to oligonucleotides was validated by disulfide reduction of Polycefin, separation of free protein and MORPH-AON by SEC–HPLC, and assessment of the amounts of MORPH-AON and protein on the basis of standardized A_{260} and the results of protein measurements. Freeze-dried Polycefin was colorless, nonhygroscopic, odorless, and stable at room temperature. The material was highly soluble in PBS and then stable for several days to weeks at 4 °C or at least 24 h at 37 °C. Polycefin had an UV-absorbance spectrum with a maximum at wavelengths <220 nm and a broad shoulder at 250–285 nm. The spectrum is indicative of carboxyl esters, carboxyamides, carboxylate, oligonucleotides, and protein. Dye-Polycefin showed also the absorbance and the fluorescence of the conjugated dye.

Analysis of Polycefin by Nonreducing SDS–PAGE

Sodium dodecyl sulfate polyacrylamide gel electrophoresis (SDS–PAGE) of Fluorescein-Polycefin was performed to identify the number of mAb molecules (shown is the result with mAb OX-26) conjugated with the PMLA scaffold (Figure 1). A single band of conjugated mAb of approximately 150 kDa was revealed under nonreducing conditions. Bands of higher molecular masses were not observed excluding the possibility of multiplets of conjugated IgG's.

To visualize which of the IgGchains were conjugated to the scaffold, samples were examined by SDS–PAGE under reducing conditions, and results were compared with those for unsubstituted mAb OX-26. Western blots, Fluorescein-dependent fluorescence, and protein staining (Coomassie Brilliant Blue) revealed bands of variable intensities in the range of 50 kDa and 62 kDa that referred to the intact H-chain and a main proteolytic fragment of mAb OX-26 (lanes R1 and R5) and Fluorescein-Polycefin (lanes R2–R4). L-Chains (25 kDa) were only protein stained (R4 and R5). The results indicated that PMLA was exclusively conjugated with the H-chain. It should be mentioned that the molecular mass scale by the polypeptide markers is not valid for Fluorescein-Polycefin, because the PMLA scaffold, unlike polypeptides, has little or no affinity for SDS and does not measurably affect mobility retardation.

Morpholino Oligonucleotide Release from Polycefin

To test for the function of the MORPH-AON releasing module, Polycefin was incubated with glutathione at a concentration of 3 mM typical for cytoplasm. The time dependence of the observed disulfide exchange was biphasic, indicating the release of 50% MORPH-AONs after 30 min and 70% after 60 min. The release was completed after 4 h. Mixed disulfide between MORPH-AON and glutathione was an intermediate of the exchange reaction and amounted to 30% of total free and conjugated MORPH-AONs after 10 s, 50% after 30 min, 20% after 1 h, 12% after 3 h. The results are in agreement with Polycefin structure and suggest free MORPH-AONs shortly after entry into the cytoplasm.

Membrane Disruption

The membrane disrupting feature of Polycefin was tested by the hemolytic assay typically used elsewhere for measuring this kind of effects on biological membranes (21). Experiments were performed in the pH range 5–6 typically found in endosomes maturating to lysosomes. Figure 2a shows stimulation of cell rupture by Polycefin. The contribution by mAb OX-26 (comparison of conjugates **3** and **19**) was negligible, whereas the MORPH-AONs indicated a membrane stabilizing effect (comparison of conjugates **3** and **18**). Protection module $mPEG_{5000}$-NH_2 (5–15%) (comparison of conjugates **9**–**11**) also strongly stabilized red blood cells (Figure 2b), whereas 2-MEA residues alone had no effect (results not shown). Comparison of the amino acids glycine (63%), L-alanine (56%), and L-valine (55%) (conjugates **12**–**14**) in Figure 1c revealed amino acid side chain dependent rupture that increased according to hydrophobicity. The disrupting effect of L-valine increased as a function of scaffold loading (Figure 1d, conjugates **15**–**17**). The pH-dependence is in agreement with charge neutralization by protonation of carboxylates of PMLA and amino acid residues.

Polycefin Does Not Change Cell Viability

To evaluate the cytotoxicity, we have measured cell viability after treatment with Polycefin. The relative numbers of viable cells were measured in cultures of two human gliomas, U87MG and M059K, and normal human astrocytes, HAST 040. The numbers of treated cells were compared with those of replicate cultures without treatment (taken as 100%). Cell

viability for each cell line in two separate experiments was higher than 90% (Figure 3). Untreated controls and treated cultures did not differ significantly from each other ($p>0.05$). Based on these data we concluded that Polycefin at concentration 1.4 and 14 μM did not exert toxic effects on these cell lines.

In Vitro Studies of Polycefin Cell Delivery

In the in vitro studies with human U87MG and T98G glioblastoma cell lines, we have employed Polycefin (**8**) and its variant (**18**), Polycefin without mAb to transferrin receptor [Polycefin(-mAb)], both of them Fluorescein labeled.

We first established that anti-rat mAb OX-26 conjugated to Polycefin for subsequent intracranial glioma treatment in rats did cross-react with human transferrin receptor (Figure 4A). This Polycefin was further used to examine its internalization mechanism in U87MG glioma cultures. After treatment with Fluorescein-labeled Polycefin (**7**), fluorescence was localized near the cell membrane and in early endosomes after 10 min and inside the cells after 20 min after addition of the drug (Figure 4B). When U87MG were co-stained with fluorescent endosomal marker FM 4-64 (visualized with rhodamine filter), the staining for both Fluorescein-Polycefin (**7**) and FM 4-64 was co-localized after 30 min, indicated by the yellow color after superposition of red and green (Figure 4C). If cells were pretreated for 10 min with mAb OX-26 in order to block the cell surface transferrin receptor and then incubated with Polycefin, the drug was not internalized, and fluorescence was not seen inside the cells (result not shown). These experiments suggested that Polycefin delivery into the cells occurred by the mechanism of transferrin receptor-mediated endocytosis.

Fluorescein-labeled Polycefin(-mAb) (**18**) administered at the same concentration also passed through the cell membrane but was detected only 1 h after the first appearance inside the cells of Fluorescein-labeled Polycefin (**7**), about the time when free Fluorescein itself appeared, administered at the same concentration (data not shown). At this time, the fluorescence intensity of Fluorescein-Polycefin (**7**) inside the cells was markedly higher than in the controls. It was concluded that the mechanisms underlying cell penetration of Polycefin(-mAb) (**18**) and free Fluorescein were not receptor-mediated endocytosis.

To show that Polycefin was internalized into tumor cells via transferrin receptor mediated endocytosis followed by its escape through membrane disruption, the inhibition of laminin-8 chain synthesis in vitro was studied. Polycefin efficiently blocked secretion of laminin $\alpha 4$ and $\beta 1$ chains in the culture medium of glioma cells as shown by semiquantitative Western blot analysis of conditioned culture media sampled after 6 days of culture (secreted human fibronectin served as gel loading control) as shown in Figure 5 and Table 1. In cultures treated with Polycefin (**8**) the expression of both chains was either significantly reduced ($\alpha 4$) or completely abolished ($\beta 1$). The relative contents of both chains in U87MG and T98G glioma-conditioned medium before and after treatment were further analyzed semiquantitatively after densitometry with secreted human fibronectin as reference. Laminin $\alpha 4$ chain secretion was reduced in U87MG cells by 67% and was completely abolished in T98G cells after treatment, whereas $\beta 1$ chain secretion was totally blocked in both cell lines (Table 1).

The results show that Polycefin was readily internalized by glioma cells via the transferrin receptor-mediated endocytosis mechanism, and that AON conjugated to the drug efficiently inhibited target protein expression in vitro.

Selective Accumulation of Polycefin in Tumor

To confirm that Polycefin was selectively accumulated in brain tumor, we have carried out intravenous injections into human brain tumor-bearing nude mice and monitored its distribution. In these experiments, we used Alexa-680-conjugated Polycefin variant **20** in comparison to Polycefin(-mAb) **21**. The replacement of Fluorescein by Alexa Fluor 680 was necessary, because Fluorescein-Polycefin had shown only a weak signal in preliminary imaging experiments at the border of detection and a high background in vivo. The new dye Alexa-680 has higher stability and gives stronger fluorescence intensity. Xenogen IVIS 200 imaging system was used to detect the drug distribution in whole body (not shown) and isolated mouse organs 5 min–72 h after injection. Repeated experiments have been conducted, giving qualitatively the same results as shown in typical images of whole brain in Figure 6. After 6 h, the drug signal was detected only in brain tumor and kidneys and was observed there during the whole examination time period up to 72 h. As shown in Figure 6A, 72 h after PBS perfusion Alexa-680-Polycefin-(-mAb) accumulated in tumor to some extent. However, a stronger signal was observed when Polycefin was conjugated with anti-transferrin receptor mAb (Figure 6B). Because this mAb may have also cross-reacted with human, it may have targeted the drug both to endothelial cells in the tumor and to tumor cells. Free dye administered in the same way was eliminated from the body in 1 h and did not accumulate in any organ (data not shown). In contrast, the accumulated drug could not be removed by flushing of the brain after perfusion. Polycefin(-mAb) may accumulate in tumors by EPR effect that has been reported for other high-molecular-mass drugs (49–51). The presence of the targeting anti-transferrin antibody resulted in a pronounced accumulation of the fluorescent label in the tumor to a far greater extent than seen for the antibody-free Polycefin variant. This demonstrated the importance of the receptor-mediated uptake mechanism. The results of the in vivo imaging experiment showed that Polycefin crossed BTB and accumulated in the brain tumor.

DISCUSSION

An ideal prototype of carrier system allows targeting of tumor tissue with the simultaneous delivery of more than a single kind of drugs at high site-directed concentrations. We have succeeded in synthesizing such a delivery system with a hitherto unprecedented variety of functionality. Our prototype complements commonly used HPMA copolymer in offering a biodegradable, nontoxic, and nonimmunogenic scaffold from a biological source, opening a new avenue for drug delivery without the danger of undegradable deposits and/or adverse reactions in the treated organism. This drug may be used for treating an individual patient's pathologic condition and for targeting multiple specific biomarkers in tissues and organs.

Our drug carrier composed of a multitude of low- and high-molecular-mass modules is a challenge for nanoscale synthesis. The strategy was based on the following rational: 1. Chemical activation of the PMLA scaffold at pendant carboxyl groups by virtue of the NHS-ester; 2. Exhaustive substitution of the highly reactive NHS-ester by formation of stable amide bonds with both the robust modules and with 2-mercaptoethylamine (2-MEA); 3. The coupling of the now scaffold-harbored thiols with the delicate, strictly water soluble modules such as proteins and nucleic acids; 4. High reaction yields and predictable stoichiometries; 5. Avoidance of side reactions/degradation of labile modules by employing mild reaction conditions; and 6. Simple and efficient purification of intermediates and end products.

Polymalic acid met the challenge as an optimal scaffold by several criteria: biological origin, highest optical and chemical purity, abundant pendant carboxyl groups for the attachment of a variety of residues, absence of rotational restriction around the polymer covalent bonds to achieve a minimum of molecular crowding, high solubility of the salt form in water, high

solubility of the acid form in acetone, DMF, DMSO, and *N*-methylpyrrolidone. The biodegradability of PMLA and of its modules and the absence of toxicity of the nanoconjugate building blocks proved Polycefin to be nontoxic in the cell viability assay.

The composition and average structure of Polycefin in Scheme 1 as a conjugate with functional groups (modules) is in accord with chemical analysis and with the UV/vis/fluorescence spectra. Reducing SDS–PAGE revealed that the PMLA scaffold was conjugated with a single mAb at H-chains. Features in Scheme 1 are corroborated by the results of disulfide cleavage and membrane disruption assays. A release of the oligonucleotides by disulfide exchange in the presence of glutathione verified both the chemical presence of the prodrug in Polycefin and the function of the releasing module. The membrane disrupting module was demonstrated by the effect of Polycefin and especially by the amino acid substitutions on the lysis of red blood cells, showing the importance of the hydrophobic valine side chains and of the carboxylate charge neutralization. Although the hemolysis assay did not represent an authentic test for endosomal membranes, the results qualitatively revealed the membrane stabilizing/destabilizing effects of PEG, MORPH-AONs, and amino acid conjugates.

The idea underlying the mechanisms that we have built into the structure of Polycefin was to cross BTB, enter glial tumor cells by the transferrin receptor-mediated endocytosis, and subsequently get released from endosomes by membrane destabilization. These features were successfully validated by the results of confocal microscopy and Western blotting, showing the cellular uptake of Polycefin via endosomes, the successful escape from endosomes, and the targeting of laminin chain coding antisense oligonucleotides to cytoplasm/nuclei, where they inhibited laminin protein synthesis. The mechanism of drug internalization was investigated in cultured U87MG glioma cells. It was shown that Polycefin-conjugated OX-26 anti-transferrin receptor mAb cross-reacted with human cells. This result was important for our xenogenic in vivo models to deliver the drug into both rat endothelial and human glioma cells. For mouse in vivo experiments we used Polycefin with anti-mouse/human transferrin receptor mAb. Thus, we prepared and tested Polycefin for future in vivo treatment and characterized its property for two independent species, rat and mouse, using anti-transferrin receptor mAb's recognizing these two species and cross-reacting with human for delivery into human tumors.

The function of antibody to transferrin receptor in targeting BTB and glioma cells was confirmed by the in vivo imaging experiments together with the confocal microscopic investigation of glioma cultures. These data demonstrate a substantial enhancement through antibody targeting in comparison to EPR effect-driven (3, 35) macromolecule accumulation in the implanted brain tumor.

Previously described nanoconjugate drug delivery systems, such as poly(acrylic acid) based derivatives (35), contain in most cases a single lipophilic prodrug to be released by endosomal cleavage of a tetrapeptide unit, occasionally a tissue-targeting molecule, and in some cases an endosomal membrane disrupting module, but a complex multifunctional structure such as that of Polycefin and delivering simultaneously two kinds of antisense oligonucleotides has not been reported. The delivery by a single carrier molecule of multiple drugs has the effect to enhance the simultaneous (synergistic) action of drugs as compared to the delivery of mixtures of single drugs. This principle has been borne out for MORPH-AON-1 and MORPH-AON-2 in Polycefin. The synthesis of Polycefin as a prototype drug delivery device allows the development of carriers with variant conjugates of several drugs and functional modules per single carrier molecule. The drug as a high-molecular-mass chemical compound owns the basic EPR-mediated selective accumulation in tumors together with the enhanced accumulation by antibody targeting. In principle, using Polycefin

as a prototype of multifunctional targeting system, it would be possible to achieve in the future an individual treatment of different human pathological conditions, based on molecular targets. These possibilities open interesting new therapeutic avenues.

Acknowledgments

The authors are indebted to Prof. Kiyotoshi Sekiguchi (Institute for Protein Research, Osaka University, Osaka, Japan) for kindly donating antibodies to laminin α4 chain. We thank Dr. John Young, Director of the Department of Comparative Medicine, Cedars-Sinai Medical Center, for invaluable help with IACUC protocols and animal work. The authors express their gratitude to Prof. Alexander V. Ljubimov for assisting in the preparation of the manuscript.

LITERATURE CITED

1. Moghimi SM, Hunter AC, Murray JC. Long-circulating and target-specific nanoparticles: theory to practice. Pharmacol. Rev. 2001; 53:283–318. [PubMed: 11356986]
2. Christie RJ, Grainger DW. Design strategies to improve soluble macromolecular delivery constructs. Adv. Drug Delivery Rev. 2003; 55:421–437.
3. Duncan R. The dawning era of polymer therapeutics. Nat Rev. 2003; 2:347–360.
4. Zhang Y, Zhu C, Pardridge WM. Antisense gene therapy of brain cancer with an artificial virus gene delivery system. Mol. Ther. 2002; 6:67–72. [PubMed: 12095305]
5. Vinogradov SV, Batrakova EV, Kabanov AV. Nanogels for oligonucleotide delivery to the brain. Bioconjugate Chem. 2004; 15:50–60.
6. Mineura K, Kowada M. Enhancement of 5-fluorouracil cytotoxicity by cisplatin in brain tumor cell lines. Cell Biol. Int. 1996; 20:355–357. [PubMed: 8688852]
7. Mologni L, leCoutre P, Nielsen PE, Gambacorti-Passerini C. Additive antisense effects of different PNAs on the in vitro translation of the PML/RARα gene. Nucleic Acids Res. 1998; 26:1934–1938. [PubMed: 9518485]
8. Matsumura Y, Maeda H. A new concept for macromolecular therapeutics in cancer chemotherapy: mechanism of tumoritropic accumulation of proteins and the antitumor agent SMANCS. Cancer Res. 1986; 46:6387–6392. [PubMed: 2946403]
9. Muggia FM. Doxorubicin-polymer conjugates: further demonstration of the concept of enhanced permeability and retention. Clin. Cancer Res. 1999; 5:7–8. [PubMed: 9918196]
10. Maeda H. SMANCS and polymer-conjugated macromolecular drugs: advantages in cancer chemotherapy. Adv. Drug Delivery Rev. 2001; 46:169–185.
11. Maeda H, Seymour LW, Miyamoto Y. Conjugates of anticancer agents and polymers: advantages of macromolecular therapeutics in vivo. Bioconjugate Chem. 1992; 3:351–362.
12. Seymour LW, Miyamoto Y, Maeda H, Brereton M, Strohalm J, Ulbrich K, Ducan R. Influence of molecular weight on passive tumour accumulation of a soluble macromolecular drug carrier. Eur. J. Cancer. 1995; 31A:766–770. [PubMed: 7640051]
13. Pardridge WM. Vector-mediated drug delivery to the brain. Adv. Drug Delivery Rev. 1999; 36:299–321.
14. Qian ZM, Li H, Sun H, Ho K. Targeted drug delivery via the transferrin receptor-mediated endocytosis pathway. Pharmacol. Rev. 2002; 54:561–587. [PubMed: 12429868]
15. Baselga J. The EGFR as a target for anticancer therapy — focus on cetuximab. Eur. J. Cancer. 2001; 37:S16–S22. [PubMed: 11597400]
16. Leamon CP, Reddy JA. Folate-targeted chemo-therapy. Adv. Drug Delivery Rev. 2004; 56:1127–1141.
17. Turk MJ, Reddy JA, Chmielewski JA, Low PS. Characterization of a novel pH-sensitive peptide that enhances drug release from folate-targeted liposomes at endosomal pHs. Biochim. Biophys. Acta. 2002; 1559:56–68. [PubMed: 11825588]
18. Rozema DB, Ekena K, Lewis DL, Loomis AG, Wolff JA. Endosomolysis by masking of a membrane-active agent (EMMA) for cytoplasmic release of macromolecules. Bioconjugate Chem. 2003; 14:51–57.

19. Philippova OE, Hourdet D, Audebert R, Khokhlov AR. pH-responsive gels of hydrophobically modified poly-(acrylic acid). Macromolecules. 1997; 30:8278–8285.
20. Murthy N, Robichaud JR, Tirrell DA, Stayton PS, Hoffman AS. The design and synthesis of polymers for eukaryotic membrane disruption. J. Controlled Release. 1999; 61:137–143.
21. Lackey CA, Murthy N, Press OW, Tirrell DA, Hoffman AS, Stayton PS. Hemolytic activity of pH-responsive polymer-streptavidin bioconjugates. Bioconjugate Chem. 1999; 10:401–405.
22. Cheung CY, Murthy N, Stayton PS, Hoffman AS. A pH-sensitive polymer that enhances cationic lipid-mediated gene transfer. Bioconjugate Chem. 2001; 12:906–910.
23. Murthy N, Xu M, Schuck S, Kunisawa J, Shastri N, Frechet JM. A macromolecular delivery vehicle for protein-based vaccines: acid-degradable protein-loaded microgels. Proc. Natl. Acad. Sci. 2003; 100:4995–5000. [PubMed: 12704236]
24. Friedrich B, Jung K, Lein M, Türk I, Rudolph B, Hampel G, Schnorr D, Loening SA. Cathepsins B, H, L and cysteine protease inhibitors in malignant prostate cell lines, primary cultured prostatic cells and prostatic tissue. Eur. J. Cancer. 1999; 35:138–144. [PubMed: 10211102]
25. Rodrigues PCA, Scheuermann K, Stockmar C, Maier G, Fiebig HH, Unger C, Mülhaupt R, Kratza F. Synthesis and in vitro efficacy of acid-sensitive poly(ethylene glycol) paclitaxel conjugates. Bioorg. Med. Chem. Lett. 2003; 13:355–360. [PubMed: 12882225]
26. Saito G, Swanson JA, Lee KD. Drug delivery strategy utilizing conjugation via reversible disulfide linkages: role and site of cellular reducing activities. Adv. Drug Delivery Rev. 2003; 55:199–215.
27. Greenwald RB, Choe YH, McGuire J, Conover CD. Effective drug delivery by PEGylated drug conjugates. Adv. Drug Delivery Rev. 2003; 55:217–250.
28. Otsuka H, Nagasaki Y, Kataoka K. PEGylated nanoparticles for biological and pharmaceutical applications. Adv. Drug Delivery Rev. 2003; 55:403–419.
29. Arpicco S, Dosio F, Bolognesi A, Lubelli C, Brusa P, Stells B, Ceruti M, Cattel L. Novel Poly(ethylene glycol) derivatives for preparation of ribosome-inactivating protein conjugates. Bioconjugate Chem. 2002; 13:757–765.
30. Maruyama K, Takahashi N, Toshiaki T, Nagaike K, Iwatsuru M. Immunoliposomes bearing poly(ethylene glycol)-coupled Fab' fragment show prolonged circulation time and high extravasation into targeted solid tumors in vivo. FEBS Lett. 1997; 413:177–180. [PubMed: 9287139]
31. Kopecek J, Kopecková P, Minko T, Lu Z. HPMA copolymer-anticancer drug conjugates: design, activity, and mechanism of action. Eur. J. Pharm. Biopharm. 2000; 50:61–81. [PubMed: 10840193]
32. Lu ZR, Shiah JG, Sakuma S, Kopecková P, Kopecek J. Design of novel bioconjugates for targeted drug delivery. J. Controlled Release. 2002; 78:165–173.
33. David A, Kopecková P, Minko T, Rubinstein A, Kopecek J. Design of a multivalent galactoside ligand for selective targeting of HPMA copolymer-doxorubicin conjugates to human colon cancer cells. Eur. J. Cancer. 2004; 40:148–157. [PubMed: 14687799]
34. Ulbrich K, Subr V. Polymeric anticancer drugs with pH-controlled activation. Adv. Drug Delivery Rev. 2004; 56:1023–1050.
35. Satchi-Fainaro R, Puder M, Davies JW, Tran HT, Samson DA, Greene AK, Corfas G, Folkman J. Targeting angiogenesis with a conjugate of HPMA copolymer and TNP-470. Nat. Med. 2004; 10:255–261. [PubMed: 14981512]
36. Lee, BS.; Vert, M.; Holler, E. Water-soluble aliphatic polyesters: poly(malic acid)s.. In: Doi, Y.; Steinbuechel, A., editors. Biopolymers. Volume 3a: Polyesters I. Wiley-VCH; New York: 2002. p. 75-103.Chapter 3
37. Ljubimova JY, Lakhter AJ, Loksh A, Yong WH, Riedinger MS, Miner JH, Sorokin LM, Ljubimov AV, Black KL. Overexpression of α4 chain-containing laminins in human glial tumors identified by gene microarray analysis. Cancer Res. 2001; 61:5601–5610. [PubMed: 11454714]
38. Fujita M, Khazenzon NM, Bose S, Sekiguchi K, Sasaki T, Carter WG, Ljubimov AV, Black KL, Ljubimova JY. Overexpression of β1 chain-containing laminins in capillary basement membranes of human breast cancer and its metastases. Breast Cancer Res. 2005; 7:411–421.
39. Khazenzon NM, Ljubimov AV, Lakhter AJ, Fujita M, Fujiwara H, Sekiguchi K, Sorokin LM, Petäjäemi N, Virtanen I, Black KL, Ljubimova JY. Antisense inhibition of laminin-8 expression

reduces invasion of human gliomas in vitro. Mol. Cancer Ther. 2003; 2:985–994. [PubMed: 14578463]

40. Summerton J, Weller D. Morpholino antisense oligomers: Design, preparation and properties. Antisense Nucleic Acid Drug Dev. 1997; 7:187–195. [PubMed: 9212909]
41. Jefferies WA, Brandon MR, Williams AF, Hunt V. Analysis of lymphopoietic stem cells with a monoclonal antibody to the rat transferrin receptor. Immunology. 1985; 54:333. [PubMed: 2981766]
42. Skarlatos S, Yoshikawa T, Pardridge WM. Transport of ^{125}I-transferrin through the rat blood-brain barrier. Brain Res. 1995; 683:164–171. [PubMed: 7552351]
43. Thorstensen K, Romslo I. The transferrin receptor: its diagnostic value and its potential as therapeutic target. Scand. J. Clin. Lab Invest. 1993; 53:113–120.
44. Singh M. Transferrin as a targeting ligand for liposomes and anticancer drugs. Curr. Pharm. Des. 1999; 5:443–451. [PubMed: 10390608]
45. Broadwell RD, Baker-Cairns BJ, Frieden PM, Oliver C, Villegas JC. Transcytosis of protein through the mammalian cerebral epithelium and endothelium III. Receptor-mediated transcytosis through the blood-brain barrier of blood-borne transferrin and antibody against the transferrin receptor. Exp. Neurol. 1996; 142:47–65. [PubMed: 8912898]
46. Carlsson J, Drevin H, Axen R. Protein thiolation and reversible protein—protein conjugation. Biochem. J. 1978; 173:723–737. [PubMed: 708370]
47. Arora V, Knapp DC, Smith BL, Stadtfield ML, Stein DA, Reddy MT, Weller DD, Iversen PL. c-Myc antisense limits rat liver regeneration and indicates role for c-myc in regulating cytochrome P-450 3A activity. J. Pharmacol. Exp. Ther. 2000; 292:921–928. [PubMed: 10688605]
48. Fujiwara H, Kikkawa Y, Sanzen N, Sekiguchi K. Purification and characterization of human laminin-8. Laminin-8 stimulates cell adhesion and migration through $\alpha_3\beta_1$ and $\alpha_6\beta_1$ integrins. J. Biol. Chem. 2001; 276:17550–17558. [PubMed: 11278628]
49. Duncan R. The dawning era of polymer therapeutics. Nat. Rev. Drug. Discovery. 2003; 2:347–360.
50. Nori A, Kopecek J. Intracellular targeting of polymer-bound drugs for cancer chemotherapy. Adv. Drug Delivery Rev. 2005; 57:609–636.
51. Duncan R, Vicent MJ, Greco F, Nicholson RI. Polymer-drug conjugates: towards a novel approach for the treatment of endrocine-related cancer. Endocr. Relat. Cancer. 2005; 12(Suppl. 1):S189–199. [PubMed: 16113096]

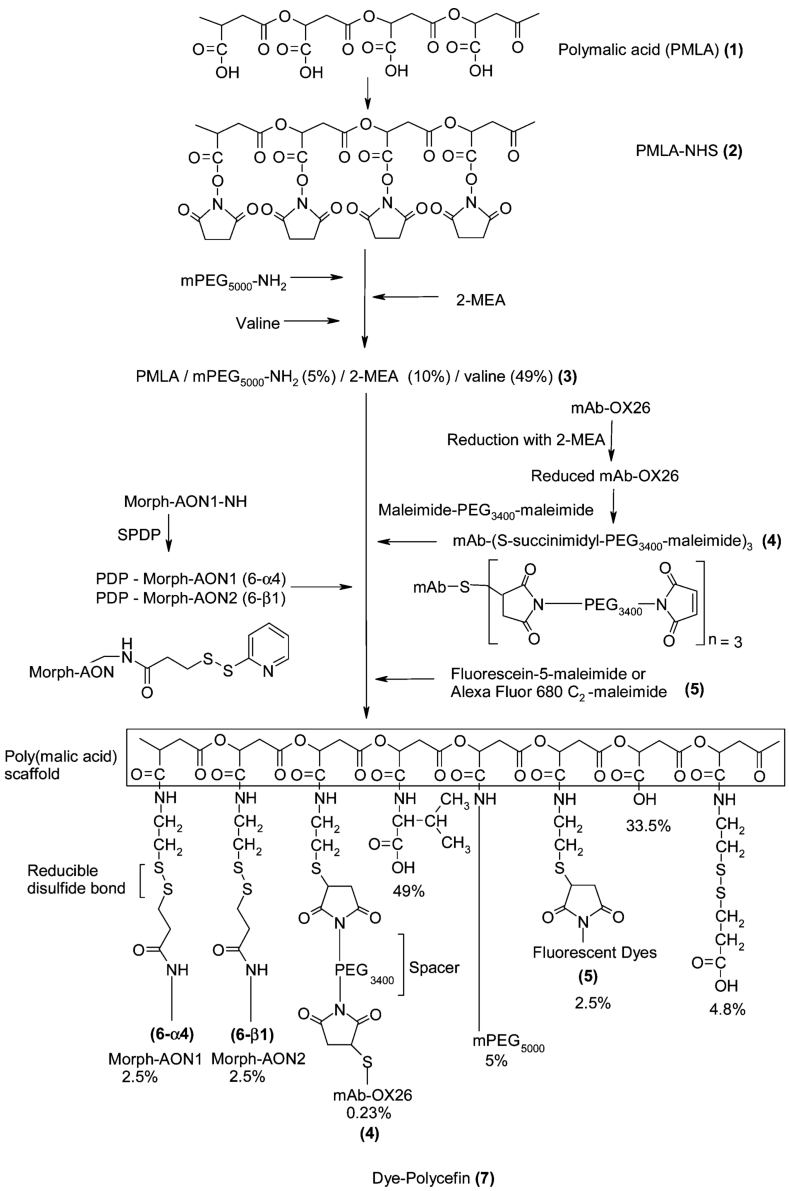

[a] Intermediates of the synthesis and of various modules are abbreviated by underlined numbers. Percent values refer to the number of malyl moieties of PMLA that are conjugated with a given module (100% = total malyl content). Polycefin (**8**) was synthesized with the omission of the fluorescent dye **5**. The distribution of conjugates along the scaffold is assumed to be random. Abbreviations are: PMLA, β-poly(L-malic acid); PMLA-NHS, *N*-hydroxysuccinimidyl ester at pending carboxyl groups of PMLA; $mPEG_{5000}$, methoxy poly(ethylene glycol) (5000 Da); 2-MEA, 2-mercaptoethylamine; mAb OX-26, mouse monoclonal antibody to rat transferrin receptor; maleimide-PEG_{3400}-maleimide, a bifunctional maleimide derivative of PEG (3400 Da); MORPH-AON-1, morpholino antisense oligonucleotide to laminin α4 chain; MORPH-AON-2, morpholino antisense oligonucleotide to laminin β1 chain.

Scheme 1.
Summary of the Synthesis of Dye-Polycefin (7)[a]

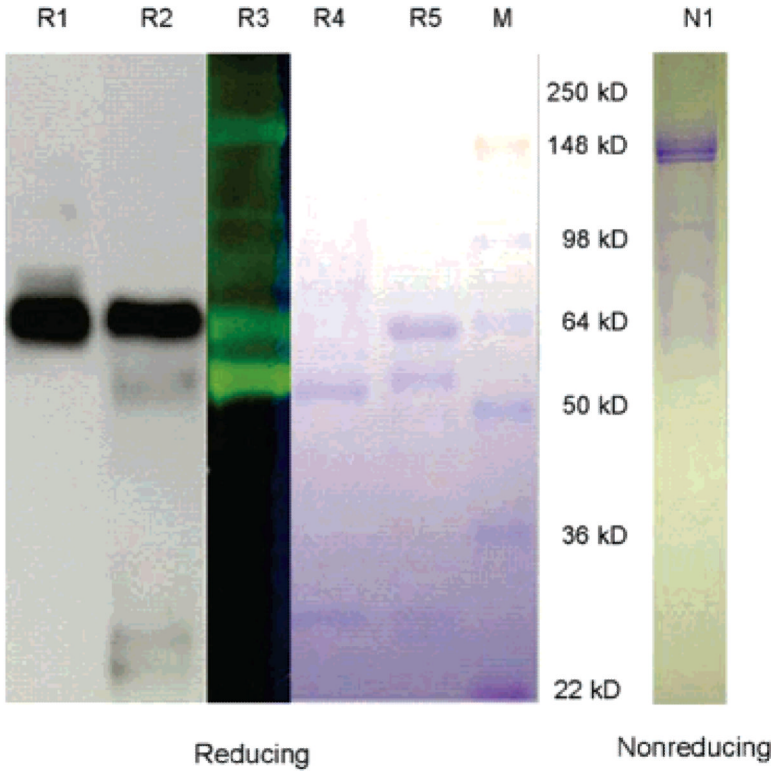

Figure 1.
SDS–PAGE of mAb OX-26 and Fluorescein-Polycefin to demonstrate the conjugation of PMLA with the H-chain of the antibody, and the absence of multiple cross-linking of antibody. Lane N1, Fluorescein-Polycefin. Electrophoresis under nonreducing condition (DTT absent) showing the integral mAb after staining with Coomassie Brilliant Blue. Only the monomeric (150 kDa) but no multiple cross-linked mAbs (>150 kDa) are seen. Lanes R1–R5 and M, electrophoresis under reducing conditions (20 mM DTT) favoring dissociation into H- and L-chains. Detection of mAb OX-26 and its H-chains by Western blotting in lanes R1 and by Coomassie Brilliant Blue staining in lane R5. Detection by Western blotting in lane R2, by Fluorescein-specific fluorescence in lane R3, and by Coomassie Brilliant Blue in R4. Lane M, molecular mass markers. Bands in positions 150–165 kDa (R1–R5) refer to H-chain or a large fragment after a limited proteolytic nicking of the samples. Bands of approximately 25 kDa (R4 and R5) refer to L-chain. Fluorescence of the H-chain (fragment) in lane R3 indicates that this chain is conjugated with the scaffold.

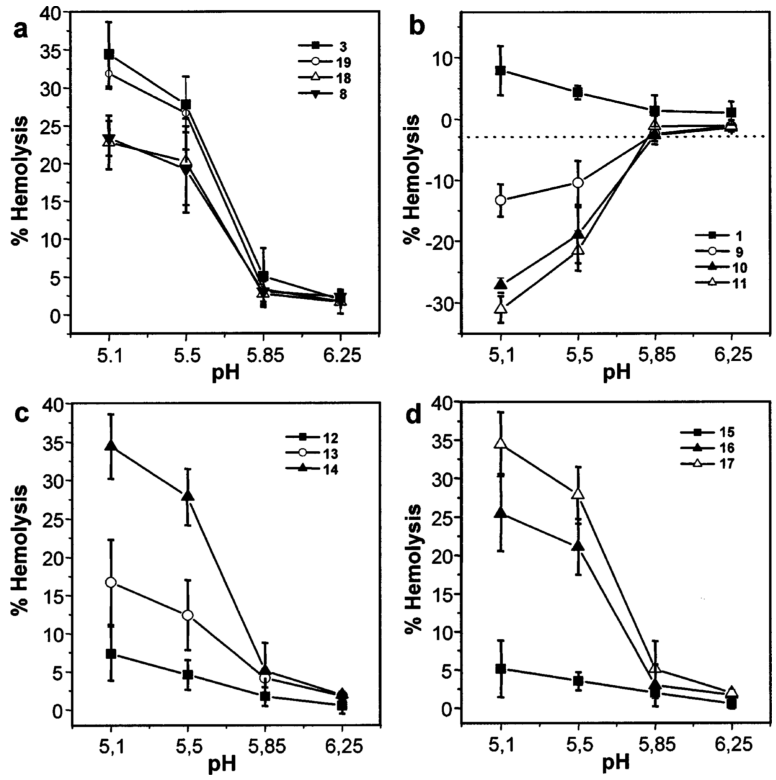

Figure 2.

Comparison of the membrane disrupting activities of the Polycefin constituents measured by the hemolysis assay. Concentrations of tested conjugates were adjusted to 1.5×10^7 molecules per red blood cell. For referring numbers to conjugate compositions see Scheme 1 and text. Panel a, effects of the antibody and the oligonucleotides. **8**, Polycefin; **3**, Polycefin without antibody and oligonucleotides, **18**, Polycefin without antibody; **19**, Polycefin without oligonucleotides. Panel b, effect of $mPEG_{5000}$ at different loads. Unsubstituted PMLA **1** and 5% (**9**), 10% (**10**) or 15% (**11**) $mPEG_{5000}$. Panel c, effect of the hydrophobicity of the amino acid side chain. Glycine (**12**), L-alanine (**13**), or L-valine (**14**). Panel d, effect of different loads of valine. 13% (**15**), 34% (**16**), 55% (**17**) L-valine.

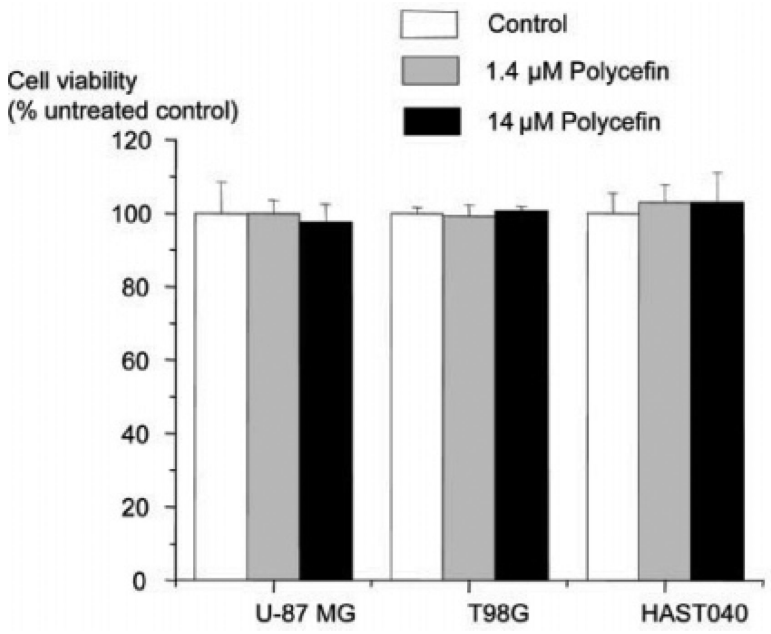

Figure 3.

Cell viability of normal (HAST040) and malignant (U87MG and T98G) astrocyte cell culture after 48 h of Polycefin incubation. Different concentrations of Polycefin (1.4 μM and 14 μM) did not change the cell viability ($p > 0.05$) after 24 h (not shown) and 48 h treatment. 100% refers to conditions without treatment (control). Cell viability was measured twice in triplicates.

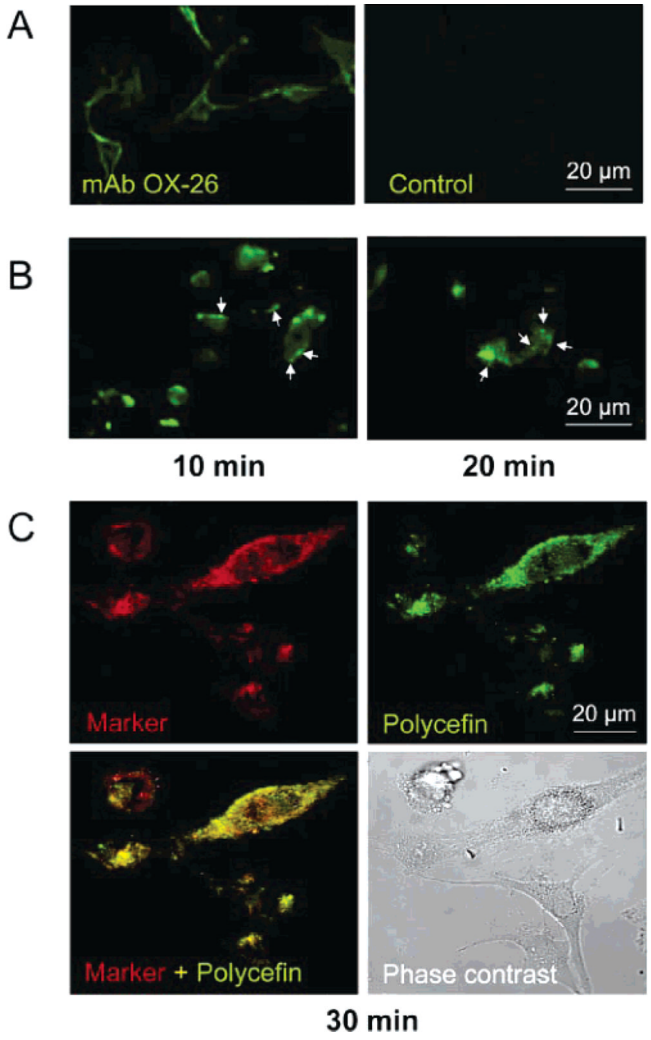

Figure 4.

Drug delivery into cultured human glioma U87MG cells. A. U87MG glioma cells display surface staining with OX-26 antibody by indirect immunofluorescence demonstrating cross-reactivity with human antigen (left). Omission of primary antibody abolished staining (negative control, right). B. Left, 10 min of U87MG treatment with Fluorescein-labeled Polycefin. The location of Polycefin is indicated by green fluorescence near the cell membrane (arrows), and early endosomes are beginning to form. Right, endosomal formation after 20 min treatment with Polycefin. Maturing endosomes are visible inside the cells (arrows). C. Co-distribution of endosomal marker FM 4-64 (marker) with Fluorescein-Polycefin (30 min) in cultured U87MG cells 30 min after treatment. FM 4-64 stains endosomes (red color), and Polycefin is found in the same place (green color). Co-localization is revealed as yellow color (lower left). Confocal microscopy.

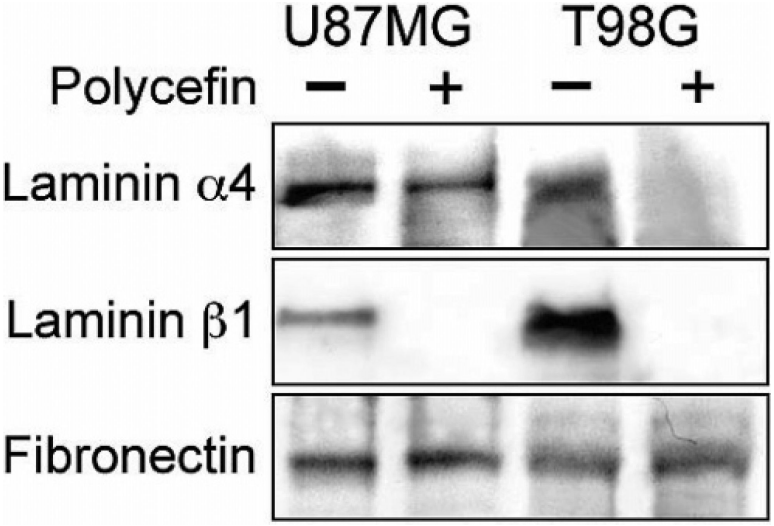

Figure 5.
In vitro targeting and inhibition of laminin chain synthesis by Polycefin. Western blot analysis of laminin chain secretion into medium with or without Polycefin treatment. Conditioned media of both glioma cell lines, U87MG and T98G, contain α4 and β1 chains of laminin-8. Polycefin markedly inhibited secretion of both laminin chains, especially of β1 chain. Gel loading was normalized by the content of secreted fibronectin.

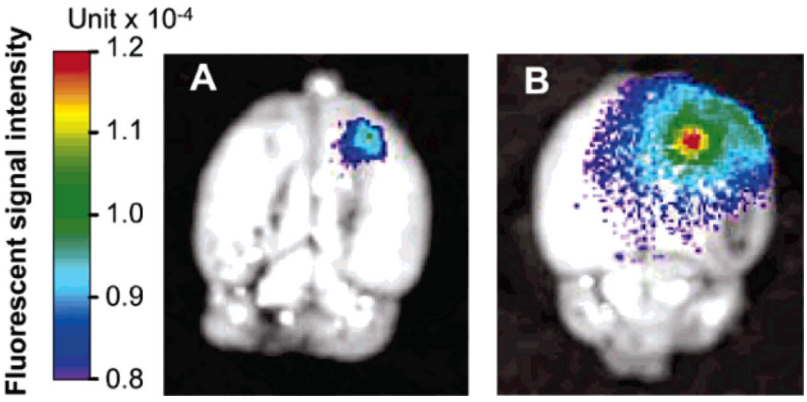

Figure 6.

Xenogen IVIS 200 imaging of Polycefin in brain glioma. Polycefin variants **20** and Polycefin(-mAb) **21** are fluorescence labeled with Alexa Fluor 680, and the valine residue (Scheme 1) is replaced by L-leucine ethyl ester. Without targeting antibody, the drug still accumulates in tumor 72 h after intravenous injection (A). Complete Polycefin with mouse targeting antibody shows significantly higher tumor retention by both amount and area (B). Imaging was carried out after flushing perfused brains with sodium-buffered saline.

Table 1

Densitometric Evaluation of Western Blot Signal Intensities for Selected Proteins in Glioma-Conditioned Media with and without Polycefin Treatment[a]

	U87MG glioma cell line			T98G glioma cell line		
protein	**control**	**treated**	**OD ratio**	**control**	**treated**	**OD ratio**
laminin α4	924	301	0.33	675.5	0	0
laminin β1	187	0	0	2387.9	0	0
fibronectin	1014	1166	1.15	720.4	754.4	1.05

[a]Control, without Polycefin; Treated, with Polycefin; OD, optical density; OD ratio, treated/control